Continental Shelf Research 30 (2010) 1019–1029

Contents lists available at ScienceDirect

Continental Shelf Research

journal homepage: www.elsevier.com/locate/csr

Reviews

Effect of submerged aquatic vegetation on turbulence induced by an oscillating grid

Dolors Pujol*, Jordi Colomer, Teresa Serra, Xavier Casamitjana

Department of Physics, Escola Politècnica – II, Campus Montilivi, 17071 Girona, Spain

ARTICLE INFO

Article history:
Received 16 September 2009
Received in revised form
11 February 2010
Accepted 25 February 2010
Available online 6 March 2010

Keywords:
Wetlands
Oscillating grid
Model canopies
Submerged aquatic vegetation
Turbulence
Sheltering

ABSTRACT

In wetlands wind-induced turbulence significantly affects the bottom boundary, and the interaction between turbulence and plant canopies is therefore particularly important. The aim of this study is to advance understanding of the impact of this interaction in submerged aquatic vegetation (SAV)[1] on vertical mixing in a fluid dominated by turbulence. Wind-generated turbulence was simulated in the laboratory using an oscillating grid. We quantify the vertical distribution of turbulent kinetic energy (TKE)[2] above and within different types of vegetation, measured by an acoustic Doppler velocimeter. Experimental conditions are analysed in two canopy models (rigid and semi-rigid) with seven solid plant fractions (SPFs)[3], three stem diameters (d)[4] and three oscillation grid frequencies (f)[5] and four natural SAVs (*Cladium mariscus, Potamogeton nodosus, Myriophyllum verticillatum and Ruppia maritima*).

Our observations suggest that the TKE above the constructed canopies was higher than that found without plants. The vertical profile varied according to the diameters of the individual stems and the SPF. Within the canopies, two zones could be distinguished. The 'transition zone', situated a few centimetres below the top of the canopy, was characterised by a reduction in the TKE. Below the transition zone, the TKE progressively decayed as the stems dissipated the turbulence, creating a zone where the TKE was lower than in the zone without stems. This is a well-known effect of SAV on turbulence, called sheltering or dampening. This phenomenon was enhanced by a decrease in the stem diameter and an increase in the SPF of the canopies, due to the reduction of the plant-to-plant distance. We have, therefore, not only observed a sheltering, but quantified it. The development of the sheltering slowed as the frequency increased, because the vegetation could not prevent the penetration of the turbulence. In the semi-rigid model, no transition zone was found inside the canopies, while sheltering was found from the very top of the plants and was intensified inside the canopies. Finally, sheltering for SAVs was similar to sheltering produced by semi-rigid plants with widespread sheltering inside the canopy.

Contents

* Corresponding author. Tel.: +34 972 41 96 27; fax: +34 972 41 80 98.
E-mail address: mdolors.pujol@udg.edu (D. Pujol).

[1] SAV: submerged aquatic vegetation.
[2] TKE: turbulence kinetic energy.
[3] SPF: solid plant fraction.
[4] *d*: stem diameter.
[5] *f*: oscillation grid frequency.

0278-4343/$ - see front matter © 2010 Elsevier Ltd. All rights reserved.
doi:10.1016/j.csr.2010.02.014

1. Introduction

Wetlands are distributed globally, covering ~4% of the Earth's land surface (Prigent et al., 2001) and producing 2000 g/m^2/year of net primary production (22.6% of the Earth's total) (Begon et al., 1986). Even so, the world may have lost 50% of all its wetlands, mostly those used for agriculture, since 1900. SAV has numerous ecological functions, with some of the most important being flood storage and desynchronisation, but which all give structural support to food web development, increase the availability of the habitat, facilitate wastewater treatment from industrial, agricultural and municipal sources and help to store greenhouse gases (Gorham, 1991; Machate et al., 1997; Willems et al., 1997; Brooks, 1989). The vegetation can also regulate the abiotic condition of light, the temperature and the dissolved oxygen (Mazzella and Alberte, 1986).

Much research has been carried out to understand the effect of emergent (Nepf, 1999; Serra et al., 2004) and submerged canopies, either in laboratory flumes or in the field (Ackerman and Okubo, 1993; Koch and Gust, 1999; Sand-Jensen and Pedersen, 1999). With submerged plants in the laboratory, natural (Gambi et al., 1990; Jarvela, 2002) and artificial (Poggi et al., 2004; Ghisalberti and Nepf, 2006; Peralta et al., 2008) plants have been used. In all cases, submerged aquatic vegetation investigations indicate that, compared with unvegetated areas, the velocity of the flow is reduced through the canopy (Gambi et al., 1990; Ackerman and Okubo, 1993; Koch and Gust, 1999), causing a reduction in TKE and enhancing sedimentation (Leonard and Croft, 2006). Studies of sedimentation demonstrate that properties like plant density (Leonard and Croft, 2006; Bouma et al., 2007), and the height (Shi et al., 1995; Nepf and Vivoni, 2000), morphology (Leonard and Reed, 2002; Morris et al., 2008) and flexibility (Ghisalberti and Nepf, 2006; Peralta et al., 2008) of the stem cause the velocity of sedimentation and the concentration of flocs to vary. Eddies found inside the canopy are produced as a result of mechanical turbulence produced by the plants and transmitted downwards. This mechanical turbulence is caused by the wake turbulence generated locally by the stems, and the shear turbulence generated by the local velocity gradient (Neumeier and Amos, 2006; Neumeier, 2007). In this case, turbulence generated by wake production has a length scale equal to that of the canopy characteristics, much smaller than the characteristic length scale of shear-generated turbulence and quickly dissipated to heat (Raupach and Thom, 1981).

Many experiments have used wind or water tunnels to obtain isotropic turbulence. In these cases, however, the generated turbulence decayed rapidly and was subjected to significant time-mean motion. Desilva and Fernando (1994) demonstrated that an oscillating grid induces turbulence, and can be used as an alternative to wind tunnel experiments since this device produces isotropic turbulence with zero mean flow and with the essential properties of the turbulence (its length and velocity scales) being determined by grid geometry, the amplitude and frequency of oscillation and the distance from the grid (Nokes, 1988). The mechanical energy in the system is converted to TKE through grid oscillation (Matsunaga et al., 1999). According to Desilva and Fernando (1994), a region is produced where turbulence is generated by jet and wake structures formed by the nature of the oscillation grid and corresponding to the open areas and the grid bars, respectively. In this region the mean shear induced by the jets and wakes becomes insignificant because they merge into one another. The turbulence quantities close to the grid are expected to be statically stationary (Holzner et al., 2006). Furthermore, the turbulence may be considered isotropic, and the corresponding measurements are often compared with predictions from theories of isotropic turbulence (Desilva and Fernando, 1994). Therefore, the design is well able to individualise the effect of turbulence, as the mean flow within the system is zero. That is of major interest in wetlands where turbulence induced by the wind is sometimes the only agent affecting the bottom boundary, and the study of the specific interaction between turbulence and plant canopies is particularly significant.

The turbulence generated by the grid has been extensively studied, both theoretically and experimentally, in the laboratory. The design has been used in the investigation of many scientific and engineering problems, such as the study of the resuspension of sediment and transport (Orlins and Gulliver, 2003), the mixing across density interfaces in stratified flows like thermoclines or haloclines (Hopfinger and Toly, 1976; Nokes, 1988), the mass transfer across a shear-free water–air interface (Brumley and Jirka, 1987), the aggregation dynamics in natural and engineered systems (Serra et al., 2008) and the desorption of contaminants from sediment (Connolly et al., 1983).

Our experiments are aimed at studying the feedback vegetation characteristics between oscillating grid turbulence (OGT)[6] and SAVs in terms of a wide variety of parameters, such as stem diameter, solid plant fraction and plant rigidity, which can mimic processes in the field. The study therefore complements other experiments carried out on channel systems.

2. Materials and methods

2.1. Experimental device

The experiments were conducted with an OGT (Fig. 1a) that consisted of a Plexiglas box with interior dimensions of $28 \times 28 \times 49$ cm^3. A Plexiglas grid was fitted over the top of the tank at a distance of $z_0 = 0.02$ m from the water surface (Fig. 1b). The square, 1 cm thick grid was composed of 5×5 bars, with a width between the bars of (M)[7] $= 0.05$ m for a mesh spacing corresponding to a solidity of 31% (defined as the fractional solid area occupied by bars). It was placed horizontally and oscillated vertically with a fixed stroke of s[8] $= 0.05$ m, and variable frequencies of $f = 0.8$, 1.6 and 2.8 Hz. A clearance of 5 mm between the sidewalls and the grid was maintained. The grid was suspended inside the tank at a height of 0.365 m from the tank bottom and was driven by a variable-speed motor located outside the tank.

[6] OGT: oscillating grid turbulence.
[7] M: spacing between bars in oscillating grid.
[8] s: stroke.

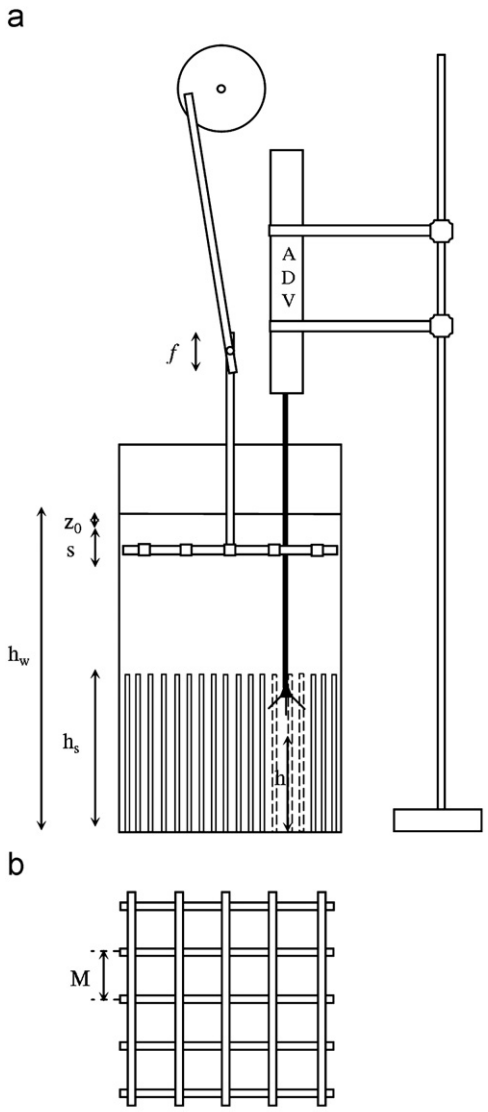

Fig. 1. Schematic view of the laboratory experiment: (a) the structure of the device used in this study, where h_w is the height of the water column (0.41 m); h_s is the height of the stem (0.17 m); s is the stroke of the grid situated at the top (0.05 m); z_0 is the distance between the water surface and the highest position of the mesh (0.02 m); h is the height of the velocity samples (0.25, 0.23, 0.21, 0.20, 0.18, 0.17, 0.16, 0.14, 0.12, 0.10, 0.08, 0.06, 0.05, 0.04 m above the bed); and f is the grid frequency (0.8, 1.6, 2.8 Hz); (b) the grid where M is the width (0.05 m).

The turbulence generated by OGT is based on grid parameters such as M and s. Variations in the horizontal (u_0,[9] v_0) and vertical (w_0[10]) RMS velocities and the integral length scale (l_0[11]) of turbulence with distance z (measured from a virtual origin) can be expressed as:

$$u_0 = C_1 s^{3/2} M^{1/2} f z^{-1} \quad (1)$$

$$v_0 = C_2 s^{3/2} M^{1/2} f z^{-1} \quad (2)$$

$$l_0 = C_3 z \quad (3)$$

where $C_1=0.22$, $C_2=0.25$ and $C_3=0.10$ are constants that depend on the grid's geometry (Desilva and Fernando, 1994; Hopfinger and Toly, 1976).

To calculate the grid's Reynolds number, Re_G[12], we used the equation of Desilva and Fernando (1994), based on $Re_G = u_0 l_0 / \nu$ and Eqs. (1) and (3):

$$Re_G = \frac{C_1 C_3 s^{3/2} M^{1/2} f}{\nu} \quad (4)$$

where ν[13] is the kinematic viscosity ($0.93 \cdot 10^{-6}$ m^2/s). This resulted in the Reynolds values for $f=0.8$, 1.6 and 2.8 Hz working out as 47, 95 and 166, respectively, from which we assumed that the flow was fully turbulent (Serra et al., 2008).

2.2. Methods of analysis

To obtain reliable velocity records, the mean quantities have to remain constant over the period of the study. For stationary velocity records, the instantaneous velocities (u,[14] v[15] and w[16]) are decomposed into the sum of time-averaged velocities (U,[17] V[18] and W[19]) and the turbulent components (u',[20] v'[21] and w'[22]), which meant the TKE could be calculated from the following equation:

$$TKE = \frac{1}{2}\rho_w \left(\overline{u'^2} + \overline{v'^2} + \overline{w'^2}\right) \quad (5)$$

where ρ_w[23] is the water density.

The TKE difference (ΔTKE)[24] between samples with and without plants was expressed as a percentage and calculated according to:

$$\Delta TKE_h = \frac{TKE_{SAV} - TKE_{noSAV}}{TKE_{noSAV}} \times 100 \quad (6)$$

where h is the height of the samples, TKE_{SAV} is the TKE measured with a canopy at height h and TKE_{noSAV} is the TKE measured without a canopy at height h.

2.3. Measuring technique

Flow velocities were recorded with an acoustic Doppler velocimeter (ADV)[25] (the Sontek/YSI 16-MHz MicroADV). The ADV has three acoustic receivers and one acoustic transmitter, and provides water velocity measurements in three directions: two horizontal flow components (u and v) and a vertical component (w). The acoustic frequency was 16 MHz, the sampling volume was 0.09 cm^3 and the distance to the sampling volume was 5 cm. The electronic noise of the measurements was smaller than the natural fluctuations caused by the turbulence. The ADV, which was operated manually, was mounted on a movable vertical frame so it could acquire single point measurements. For all experiments the ADV was placed at 7 cm of one side wall (1.4 mesh size) and at 12 cm from the other side wall (2.4 mesh size) as suggested by Orlins and Gulliver (2003), who used an oscillating grid chamber to quantify the turbulence and

[9] u_0 and v_0: horizontal RMS velocity.
[10] w_0: vertical RMS velocity.
[11] l_0: integral length scale.
[12] Re_G: Reynolds number of the grid.
[13] ν: kinematic viscosity.
[14] u: instantaneous horizontal velocity.
[15] v: instantaneous horizontal velocity.
[16] w: instantaneous vertical velocity.
[17] U: horizontal mean velocity.
[18] V: horizontal mean velocity.
[19] W: vertical mean velocity.
[20] u': horizontal turbulent velocity.
[21] v': horizontal turbulent velocity.
[22] w': vertical turbulent velocity.
[23] ρ_w: water density.
[24] ΔTKE: TKE difference between samples with and without plants at the same height.
[25] ADV: acoustic Doppler velocimeter.

sediment resuspension, with enough distance to wall to not measure their effects. In addition, the mesh endings were designed to reduce mean-secondary circulation. For each experiment, a vertical turbulence profile was taken over a height of 0.05–0.25 m, with 13 height positions in total, from the bottom of the tank.

In order to obtain valid data acquisition within the canopy, just a few stems were removed to avoid blocking the pathway of the ADV beam, as was done by Neumeier and Ciavola (2004) and Neumeier and Amos (2006). To minimise the effect of this 'hole', its shape was specifically designed to allow the ADV acoustic receivers and the acoustic transmitter to perform properly. To test the effect of the 'hole', we measured the velocities half a centimeter above the top of the canopy with and without plants. A comparison of the two measurements showed that at the highest SPF the difference was around 10% whereas at the lowest the difference was around 3%. We therefore concluded that the 'hole' contributed little to modify the hydrodynamics in that system.

The ADV instrument was configured to transmit 10 acoustic signals per second with a sampling time interval of 5 min (i.e. 3000 records per sample). The measurements were taken after oscillating the grid for about 10 mins so that the turbulence was fully established. Each measurement was repeated five times. In addition, to avoid spikes, beam correlations from ADV measurements lower than 80% were removed. Finally, time-series records were used to calculate the turbulent velocities, and the results of repeated profiles at the same point were averaged.

Table 1
Summary of the 17 different situations studied with different SPFs, diameters and canopy models (R=rigid canopy model and SR=semi-rigid canopy model).

	SPF						
d (mm)	0.6%	3%	5%	8%	10%	15%	25%
4 mm	SR	SR	R, SR	SR	R, SR	R	R
6 mm			R		R	R	R
10 mm			R		R	R	R

For each situation the oscillation frequencies were 0.8, 1.6 and 2.8 Hz. The height of the plants was 17 cm.

2.4. Vegetation quantification

The characteristics of SAV vary greatly in terms of height, stem diameter, plant density, geometry and morphology. In order to obtain features in the laboratory similar to those in the field, 51 different situations were studied featuring two different canopy models, seven SPFs, three stem diameters, and three oscillating frequencies (Table 1).

The rigid canopy model consisted of rigid cylinders made of PVC (Fig. 2a left). The density of the canopy was implemented by four different SPFs. According to Serra et al. (2004) the SPF can be defined as the fractional plant area at the bottom occupied by stems:

$$SPF = \frac{n\pi(d/2)^2}{A} \tag{7}$$

where n is the number of plants, d is the diameter of the plant and A is the total area studied. SPFs of 5%, 10%, 15% and 25% and

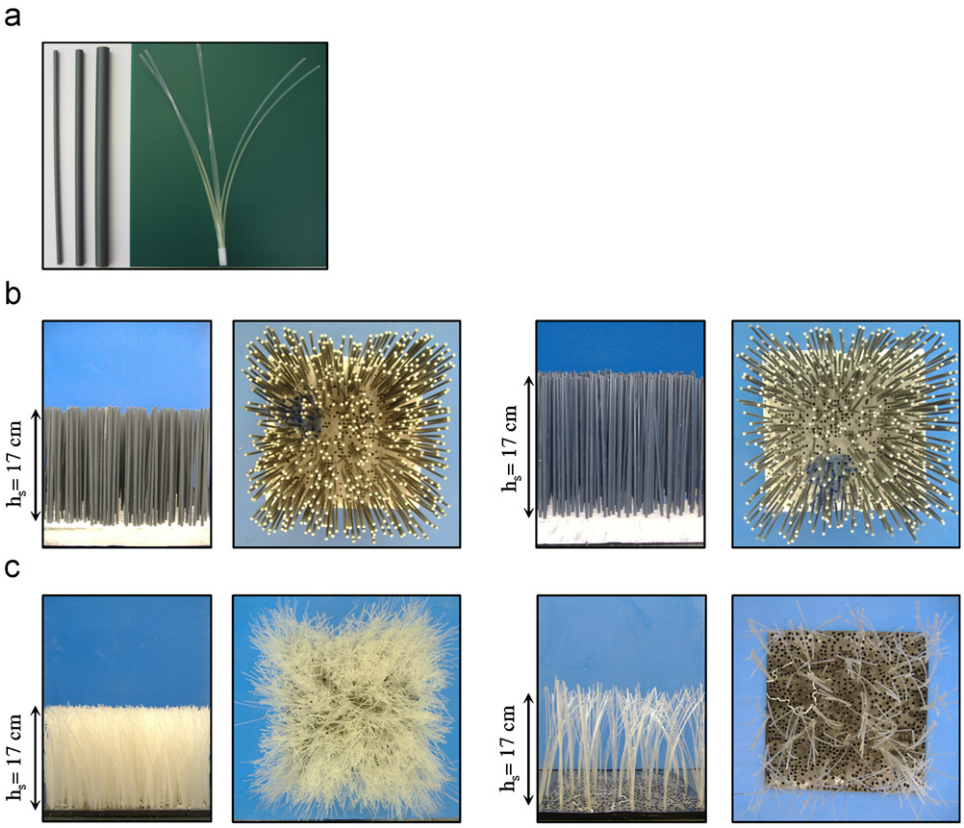

Fig. 2. Photographs of vegetation studied: (a) rigid canopy (d=10, 6 and 4 mm) on the left and semi-rigid (d=4 mm) on the right; (b) lateral and top view of the rigid canopy (on the left, SPF=10%, d=4 mm and on the right, SPF=5%, d=4 mm); (c) lateral and top view of the semi-rigid canopy (on the left, SPF=10%, d=4 mm and on the right, SPF=0.6%, d=4 mm).

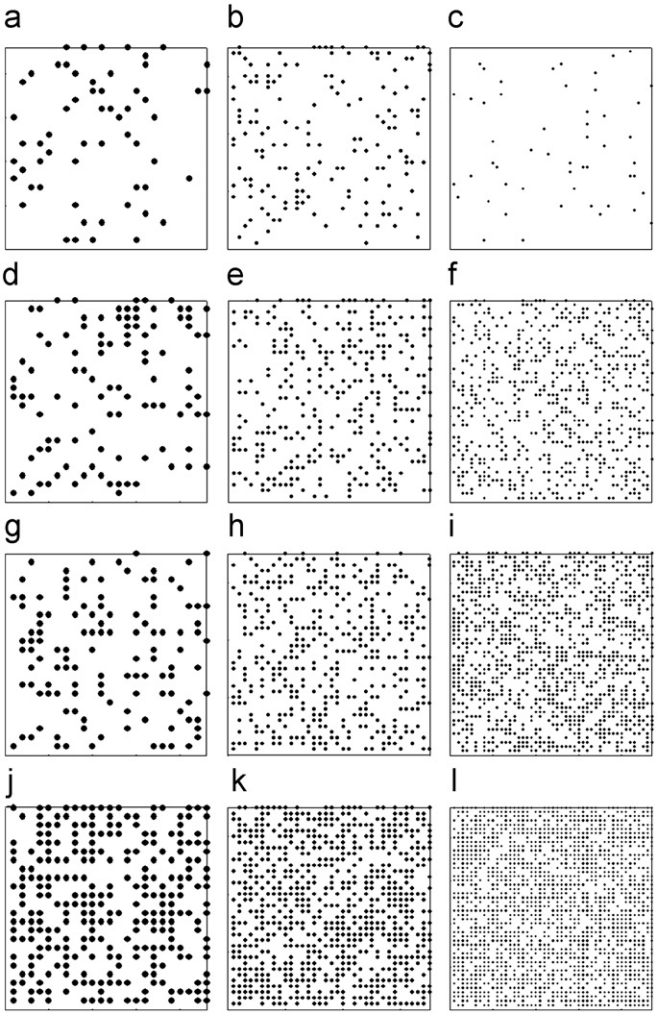

Fig. 3. A plot of distributions for each feature: (a) $d=10$ mm, SPF=5%; (b) $d=6$ mm, SPF=5%; (c) $d=4$ mm, SPF=5%; (d) $d=10$ mm, SPF=10%; (e) $d=6$ mm, SPF=10%; (f) $d=4$ mm, SPF=10%; (g) $d=10$ mm, SPF=15%; (h) $d=6$ mm, SPF=15%; (i) $d=4$ mm, SPF=15%; (j) $d=10$ mm, SPF=25%; (k) $d=6$ mm, SPF=25%, (l) $d=4$ mm, SPF=25%.

cylinder diameters of 4, 6 and 10 mm were used for this study. The distribution of each SPF was made by means of a computer randomisation function with the distributions shown in Fig. 3.

A semi-rigid canopy model was made of nylon threads each 1.6 mm in diameter (Fig. 2c). To compare semi-rigid to rigid plants at $d=4$ mm, 6 nylon threads were stacked together at the base to mimic the equivalent stem diameter. Due to the difficulty of determining SPFs with this canopy, three techniques were used for their calculation. The first was based on the application of Eq. (7) at the base of the canopy with five different SPFs (0.6%, 3%, 5%, 8% and 10%) being considered. The second was based on determining the lateral obstruction ratio obtained from a binarised black and white picture using image analysis software (Neumeier, 2005). This software was designed to distinguish between black and white zones in order to calculate the area of the canopy. In this case, the lateral obstruction was 31%, 83%, 97%, 98% and 99%. The third method consisted of calculating the vegetation cover at the top of the canopy using a similar method to that developed by Neumeier (2005). In this case, for each situation studied photographs of the top were taken with a black background (the colour was the opposite of the canopy colour). We averaged the results over five pictures to calculate that the vegetation cover at the top of the canopy was 21%, 56%, 57%, 74% and 76% (Table 2).

Table 2
Comparison of the three different techniques for measuring the SPF.

SPF (bottom view, according to Serra et al., 2004)	Lateral obstruction (lateral view according to Neumeier, 2005)	Vegetation cover (top view)
0.6%	30.9%	20.6%
3%	82.7%	55.5%
5%	96.9%	57.3%
8%	98.1%	74.4%
10%	99.1%	76%

Real plants were used to compare the results obtained with those obtained for rigid and semi-rigid plant canopies. Four real plants were used for the study: *Cladium mariscus*, *Potamogeton nodosus*, *Myriophyllum verticillatum* and *Ruppia maritima* (Fig. 4). The density of each natural plant was 459 shoots/m^2. These plants were selected to give different SPF distributions and different morphologies. All of them are submerged aquatic vegetation in their natural media, with three of them developing in freshwater environments and one in a salty environment (*R. maritima*). The plants were cut at a height of 17 cm so that results could be compared with those obtained with previous models of rigid and semi-rigid canopies. *C. mariscus* (Fig. 4a) has a similar morphology to *R. maritima*: both have stem diameters of less than 2 mm. However, while *R. maritima* leaves are narrower, *C. mariscus* leaves are stiffer and wider. *M. verticillatum* (Fig. 4b) has compound and divided leaves, like feathers, and its stem is around 4 mm in diameter. *P. nodosus* (Fig. 4c) has a long stem with wide horizontal leaves and a diameter between 4 and 5 mm. Both *P. nodosus* and *M. verticillatum* have leaves that grow at each level of the stem and perpendicular to it. In addition, the vertical SPF is distributed homogeneously through the stem. *R. maritima* (Fig. 4d) has long, narrow upward leaves and lives in salt marshes.

3. Results

The experiments with no SAV showed that TKE decreased following power decay, with the greatest values closest to the grid and decreasing towards the bottom of the tank (Fig. 5). TKE values were most different close to the grid at the different frequencies studied. Near the bottom, the results at the three frequencies studied were almost equal. The uncertainty in the data acquisition was calculated using the equation described by Kline and McClintock (1953) for the propagation of errors in physical measurements.

3.1. Experiments with the rigid canopy model

Three hydrodynamic regions with depth could be distinguished from all the TKE profiles for experiments with rigid canopies. The first was situated above the canopy, from 0.25 to 0.17 m above the bed. In all of the experiments the TKE was greater in this region than without plants (Fig. 6). The second region behaved like a transition zone and was situated below the top of the canopy to the depth where the TKE was lower than that found with no SAV. This depth depends on the stem diameter and canopy density at any depth. At the lowest diameter ($d=4$ mm), the depth of the transition zone is 0.16 m (Fig. 6c and d), but as the stem diameter increases, the transition zone is more accentuated and can reach 0.08 m when $d=10$ mm. Well inside the canopy, the TKE decayed progressively, creating a third zone

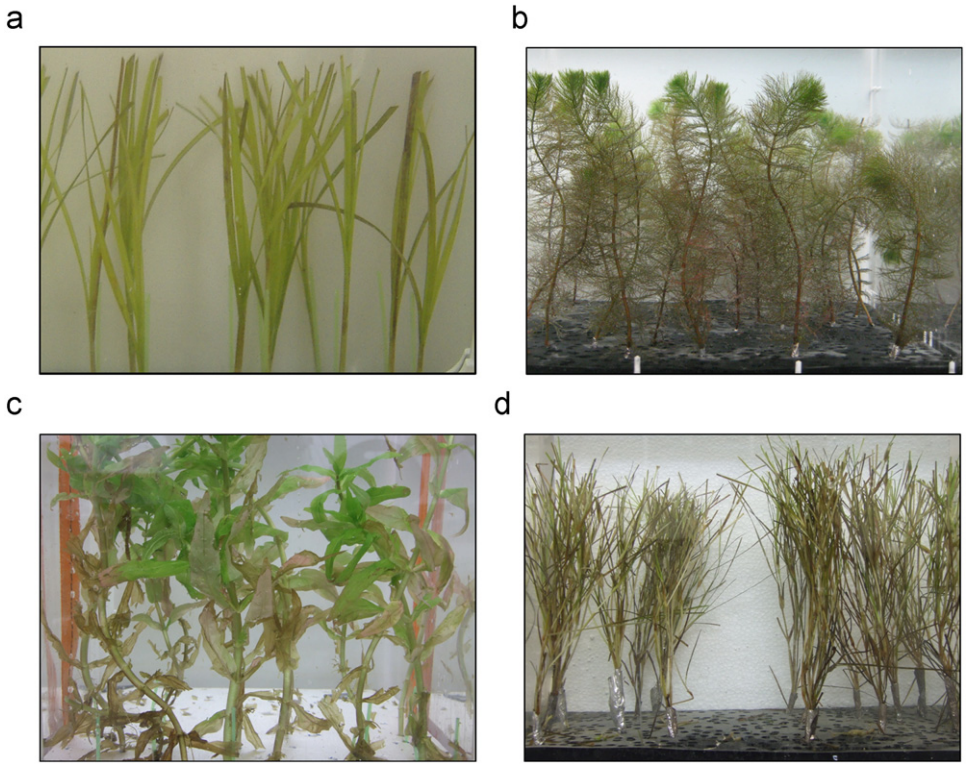

Fig. 4. Illustrations of the submerged aquatic vegetation studied: (a) *Cladium mariscus*; (b) *Myriophyllum verticillatum*; (c) *Potamogeton nodosus*; (d) *Ruppia martitima.*

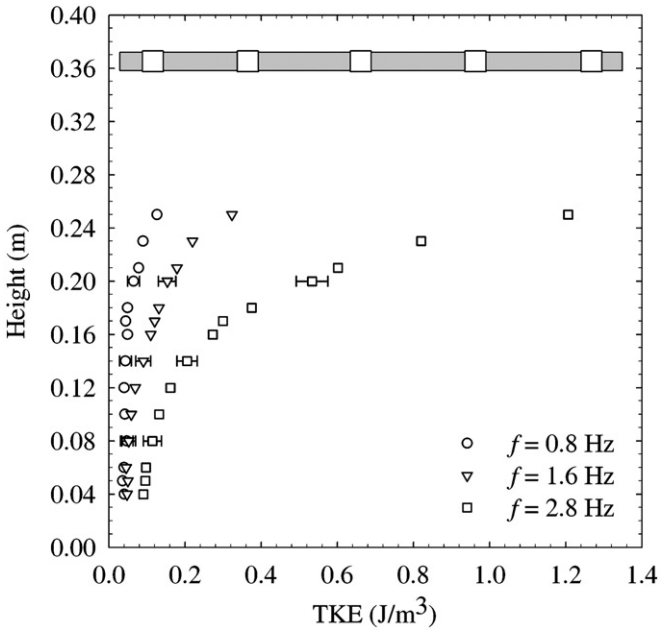

Fig. 5. TKE profile with no SAV at 0.8 (circles), 1.6 (triangles) and 2.8 Hz (squares) frequencies. The horizontal error bars represent the uncertainty of experimental *runs.*

where it was lower than that found where there was no SAV. The gradient of this zone was the lowest of the three.

One cm above the constructed canopy (hereafter $hs+1$) the ΔTKE was greatest and always positive for the largest stem diameters (56%) and the largest SPF and f (Table 3). Positive values of ΔTKE indicate a gain in TKE, and negative values indicate a decrease. Down in the canopy, the ΔTKE suffered a progressive decrease in the transition zone, one cm below the top of the canopy (hereafter $hs-1$), and well inside the canopy (hereafter $hs/2$, half the height of the stems). It was only positive for the lowest SPF (5%) and the largest stem diameter ($d=10$ mm) (Table 3). The smallest ΔTKE was found in the constructed canopy with the smallest stem diameter ($d=4$ mm) for all the SPFs and f.

Besides the stem diameter, the SPF was also found to play an important role in TKE profiles. Above the constructed canopy ($hs+1$), the greater the SPF the greater the ΔTKE (Fig. 7a). For SPF=25% it was found to be between ~2 ($d=4$ mm) and ~6 ($d=10$ mm) times larger than the ΔTKE found when the SPF was 5%. In the transition zone, 1 cm below the top of the constructed canopy ($hs-1$), the ΔTKE showed a slight decrease with an increase in the SPF, especially for the smallest diameters (Fig. 7b). Inside the constructed canopy ($hs/2$) the reduction in the TKE was greater and increased with the SPF (Fig. 7c); this relationship was found with the stems with smallest diameters. The differences in ΔTKE between $hs+1$ and $hs/2$ with all diameters were more evident with larger SPFs at all the oscillating grid frequencies (Table 3). For instance, the difference in ΔTKE above and well inside the constructed canopy at SPF=25%, $d=4$ mm and $f=2.8$ Hz was 62.9%, whereas the difference in ΔTKE between the two zones at SPF=5%, $d=4$ mm and $f=2.8$ Hz was only 3.1%.

3.2. Experiments with a semi-rigid canopy model

In contrast to the rigid model, the transition zone practically disappeared when the constructed semi-rigid canopy was used, and only two regions could be found, one above the canopy ($hs+1$), and the other well inside it ($hs/2$) (Fig. 8). Above the semi-rigid canopy ($hs+1$), the ΔTKE increased with the SPF at all three frequencies (Fig. 9a, b and c). Inside the constructed canopy ($hs/2$), the reduction in the ΔTKE was found to increase with the SPF, as was found with the rigid canopy model. For instance, the ΔTKE at $hs+1$ for SPF=10%, $d=4$ mm and $f=1.6$ Hz was found to be 16.5%,

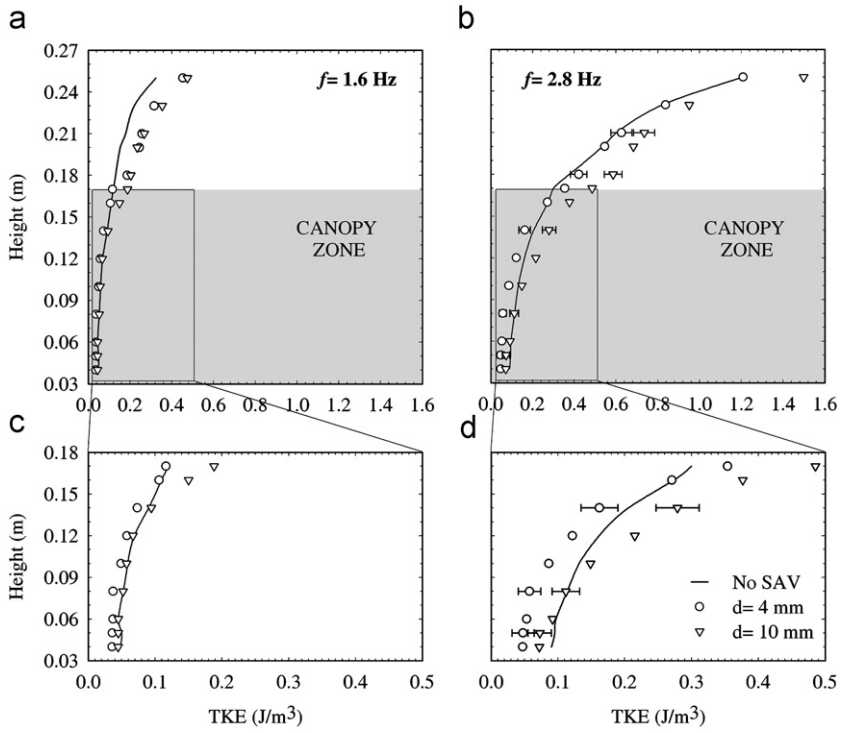

Fig. 6. TKE profiles of rigid canopy at SPF=25%, 4 (circles) and 10 mm (triangles) in diameter and with no SAV (solid line): (a) f=1.6 Hz; (b) f=2.8 Hz. Enlargement of the canopy zone: (c) f=1.6 Hz; (d) f=2.8 Hz. The horizontal error bars represent the uncertainty of experimental runs.

Table 3
The TKE difference (%) for rigid canopies at four SPFs (5%, 10%, 15% and 25%), three stem diameters (10, 6 and 4 mm), and for semi-rigid canopies at three SPFs (5%, 8% and 10%) at two frequencies (1.6 and 2.8 Hz) at three different heights (hs+1, $hs-1$ and hs/2).

			1.6 Hz			2.8 Hz		
	SPF (%)	d (mm)	h_s+1	h_s-1	h_s/2	h_s+1	h_s-1	h_s/2
Rigid canopy	5	4	19.6	27.9	−12.8	6.9	18.9	3.8
		6	20.0	35.2	−3.4	10.1	43.5	−1.9
		10	22.4	53.4	18.5	9.9	38.2	16.7
	10	4	16.5	20.0	−18.8	4.6	10.7	−31.9
		6	18.6	23.2	−1.06	12.8	28.6	−26.8
		10	24.6	41.6	−4.4	14.9	51.1	−7.6
	15	4	26.1	8.9	−26.0	6.9	0.4	−33.7
		6	40.6	21.5	−25.4	23.9	21.5	−39.5
		10	46.3	45.8	−6.4	29.5	43.3	−4.9
	25	4	42.0	−3.2	−28.8	12.2	−0.9	−50.7
		6	35.2	0.9	−30.0	29.1	25.6	−50.8
		10	55.9	37.0	−14.0	56.2	37.9	−4.2
Semi rigid canopy	5	4	25.5	−3.2	−18.2	12.2	−13.9	−34.5
	8		28.2	−5.0	−25.9	17.8	−15.0	−13.9
	10		35.7	−22.9	−34.6	36.5	−13.9	−52.9

while the ΔTKE under the same conditions for the semi-rigid canopy model was found to be around 35% (Table 3). In addition, at hs/2, the ΔTKE for the rigid canopy (with the same variables as before) was 19% (Table 3), lower than the ΔTKE for the semi-rigid canopy model (~34%). The differences between the ΔTKE in both zones (hs+1 and hs/2) were more evident as the SPF increased.

3.3. Experiments with field SAV

As shown in Fig. 10, field SAV behaved similarly to what was found with the semi-rigid constructed canopy. The vertical distribution of TKE also allowed us to describe results found with SAV in two zones: above (hs+1) and inside the SAV (hs/2). *C. mariscus* and *R. maritima* both had a TKE vertical profile close to that of the semi-rigid model. They had similar morphologies, long, narrow, upward leaves with a heterogeneous vertical distribution, with the major biomass in the upper part. Near the bottom both had less dense canopies. *M. verticillatum* and *P. nodosus* were the plants that reduced the TKE inside the canopy to the greatest extent. For instance, at $hs-1$ the reduction in the ΔTKE was more than 50% of its total. A drastic change in TKE between the two zones caused the disappearance of the transition zone. This phenomenon is shown in Fig. 11. Inside the canopy (hs/2) the reduction in ΔTKE was greatest for *P. nodosus* and *R. maritima*, especially at higher frequencies.

4. Discussion

4.1. Turbulence in submerged rigid constructed canopies

With the rigid constructed canopies, the vertical behaviour of the TKE profile allowed us to divide the flow into three zones: one above the canopy, another completely within the canopy and a transitional zone situated inside the top of the canopy. The zones were different in terms of their hydrodynamic behaviour. In our 36 experiments, the largest TKE values were found above the constructed canopies. This result, and the fact that the TKE increased with the SPF, can be explained in terms of the TKE being redistributed at a lower volume due to the presence of the constructed canopy, relative to the 'free-canopy' experiment. Most of the energy was concentrated above the canopy, and therefore the vegetation acted as a 'false rough floor' for the flow.

The results of this study suggest that within the canopy, interaction between water flow and the constructed canopies reduces the TKE measured relative to 'unvegetated' experiments.

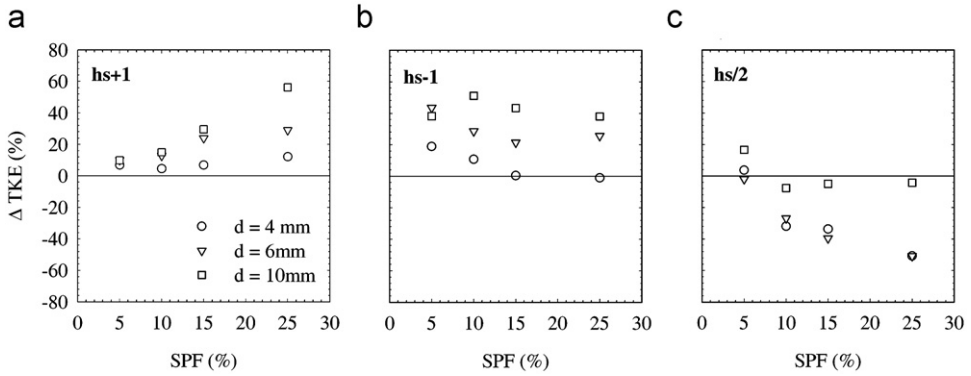

Fig. 7. TKE differences (ΔTKE) of rigid canopy at 4 (circles), 6 (triangles) and 10 mm (squares) in diameter and $f=2.8$ Hz: (a) $hs+1$; (b) $hs-1$; (c) $hs/2$.

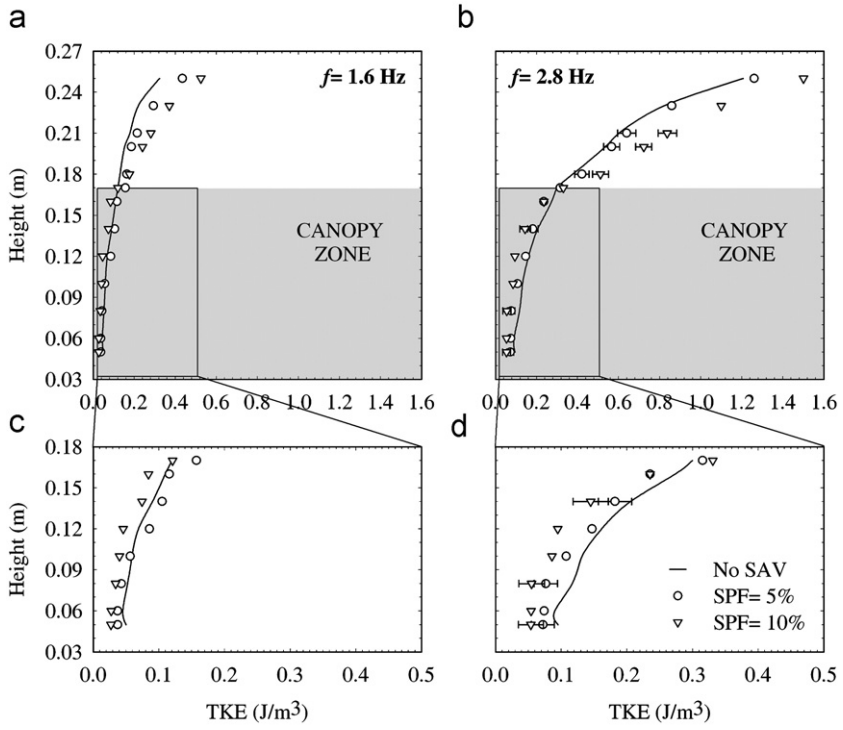

Fig. 8. TKE profiles of semi-rigid canopy at 5 (circles) and 10% (triangles) of SPF and with no SAV (solid line): (a) $f=1.6$ Hz; (b) $f=2.8$ Hz. Enlargement of the canopy zone: (c) $f=1.6$ Hz; (d) $f=2.8$ Hz. The horizontal error bars represent the uncertainty of experimental runs.

This reduction appears to be related to SPF, as others have been previously found with advection through vegetation (Nepf, 1999; Leonard and Croft, 2006). In our experiments, the depth of this zone depends on stem diameter and SPF. A reduction in the first and an increment in the second reduced the plant-to-plant distance, resulting in a reduction in the depth of the transition zone. On the other hand, well inside the constructed canopies, at $hs/2$, the SPF was not the only variable that reduced the flow; the stem diameter also played an important role in dissipating turbulence. More precisely, the reduction in turbulence, or sheltering produced by the canopy, was enhanced as the stem diameter decreased and the SPF of the canopies increased. In other words, the enhancement of the sheltering can be explained by the reduction in the stem diameter and the increment in the SPF, that both caused a reduction in the plant-to-plant distance. Nepf (1999) defined sheltering or dampening as a reduction in the in-emergent canopy macroscale diffusion due to a combination of reduced velocity and reduced eddy-scale relative to unvegetated zones. Other authors have described sheltering in the same terms as Leonard and Croft (2006) and Neumeier and Amos (2006). For example, Neumeier and Amos (2006) found a reduction in turbulence near the bed in three different vegetation types. They pointed out that this effect should enhance sediment deposition and protect the bed against subsequent erosion.

Oscillating grid frequency was the agent generating the turbulence in the system. In this system the number of eddies increases as the oscillating grid frequency increases. All through the tank, at all levels and under all experimental conditions, there was a positive relationship between oscillating frequency and TKE. The behaviour of the sheltering inside the constructed canopy for the largest SPF produced the greatest ΔTKE at any diameter and frequency, because turbulence was highly dissipated inside the dense canopy. On the other hand, the reduction in energy at low frequencies suggests that the vegetation inhibits the production of larger turbulent eddies, and it is likely that it also contributes to the breakdown of larger eddies into smaller

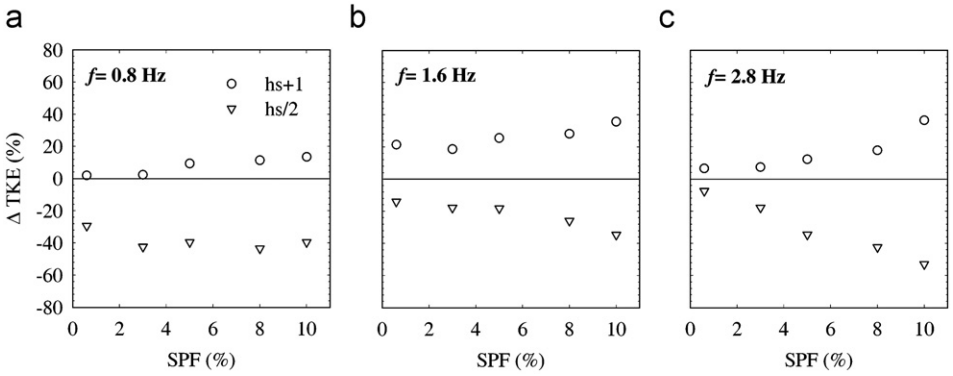

Fig. 9. TKE differences (ΔTKE) of semi-rigid canopy at *hs*+1 (circles) and *hs*/2 (triangles): (a) $f=0.8$ Hz; (b) $f=1.6$ Hz; (c) $f=2.8$ Hz.

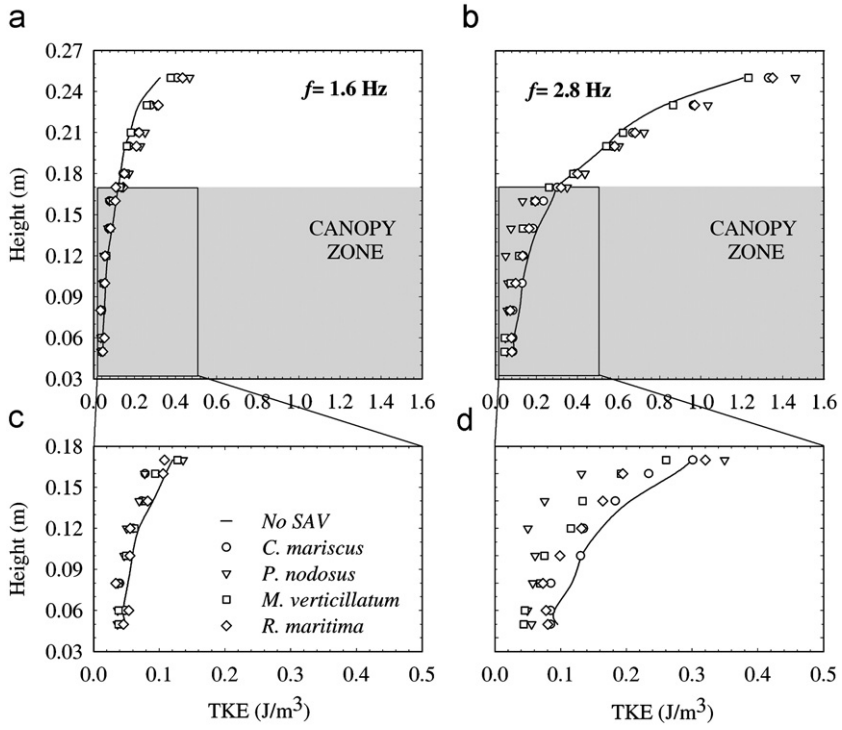

Fig. 10. TKE profiles of *Cladium mariscu* (circles), *Potamogeton nodosus* (triangles), *Myriophyllum verticillatum* (squares) and *Ruppia maritima* (diamonds) with no SAV (solid line): (a) $f=1.6$ Hz; (b) $f=2.8$ Hz. Enlargement of the canopy zone: (c) $f=1.6$ Hz; (d) $f=2.8$ Hz.

ones (Christiansen et al., 2000). At the same time, with an increase in the grid oscillating frequency, the constructed canopy cannot absorb so much energy and there is a displacement in the transmission of the energy downwards inside the canopy from the upper zone. As a result, and as shown in Table 3, the ΔTKE (%) at $hs-1$ is positive for $d=10$ mm, SPF=25% and $f=1.6$ Hz and around zero for the smallest diameters.

4.2. Turbulence in submerged semi-rigid constructed canopies

Experiments carried out with the semi-rigid model canopies showed that the transitional hydrodynamic regime disappeared, resulting in a steep gradient of TKE above and below the plants. This process was attributed to the morphology of the semi-rigid stems, where the thick stem at the base of the plant gradually divided at the top and its branches merged with the branches of its neighbours, resulting in an increase in the SPF at the top of the canopy. While the SPF obtained at the bottom of the rigid model was the same as that calculated at the top (Serra et al., 2004), the SPF calculated at the bottom of the semi-rigid SAV was completely different to the vegetation cover at the top. This shows that the role of the vegetation as a 'false rough floor' was enhanced in the semi-rigid model. More precisely, an extreme canopy condition of lateral obstruction=99% (see column 2 in Table 2) dissipated the turbulence and increased the sheltering within the canopy. Within the canopy, sheltering was also greater as the SPF increased, even at the higher oscillating grid frequencies, which is evidence of the role of vegetation controlling high energy events in the field.

4.3. Turbulence in submerged aquatic vegetation

Nepf and Vivoni (2000) showed that the bending of the canopy effectively increased the local frontal area, thereby increasing the SPF at the top of the canopy. The depth of the zone affected by the

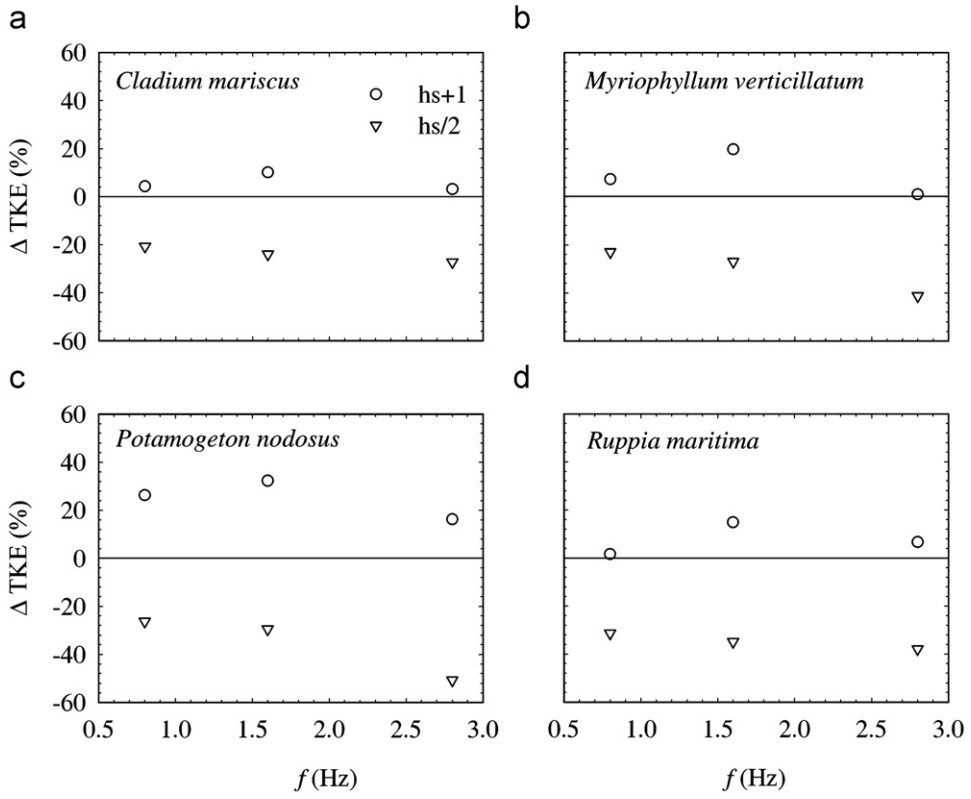

Fig. 11. TKE differences (ΔTKE) in real plants at *hs*+1(circles) and *hs*/2 (triangles): (a) *Cladium mariscus*; (b) *Myriophyllum verticillatum*; (c) *Potamogeton nodosus*; (d) *Ruppia maritima*.

sheltering was set by the depth of submergence and by canopy morphology, density and flexibility (Nepf and Vivoni, 2000). Shi and Hughes (2002) have studied the differences in plant flexibility as a stem property affecting the hydrodynamic flow. Other authors, such as Leonard and Luther (1995), Yang (1998) and Leonard and Croft (2006), have focused on the morphology of the plants and shown that the presence of elements oblique to the flow, such as leaves, inhibits the vertical transport of turbulence in the canopy.

Using SAV, the transitional zone disappeared due to the layout of the leaves, which isolated the two zones. The movement of the real plants contributed to enhancing the sheltering and resulted in the removal of the transitional zone by means of the undulating movements (Ackerman and Okubo, 1993). As the frequency increased, the sheltering intensified due to the fact that there was greater movement of the plants at the top, which incremented the attenuation of the turbulence inside the canopy. This phenomenon did not appear in either the rigid or semi-rigid canopy models as in both of these the stems did not move at all.

C. mariscus and *R. maritima* had similar TKE profiles relative to the semi-rigid constructed canopies because their design was thought to mimic this kind of natural canopy as a just step. The difference between these natural plants (Fig. 10d) is found in their flexibility. The leaves of *R. maritima* were not as stiff or as wide, so the plant bent more easily, thereby enhancing the attenuation of the TKE inside the canopy. *M. verticillatum* and *P. nodosus* were the plants that reduced the TKE inside the canopy most (Fig. 11) since they have a more complex structure. The latticework structure of the leaves of *M. verticillatum* around the stem enhanced the sheltering below. This plant had a lot of compound and divided leaves, which resulted in a featherlike structure. *P. nodosus* leaves were the widest and were positioned perpendicular to the stem. The morphology of the leaves enhanced the effect of the plants acting as a 'false rough floor', and increased the TKE gradient between the two zones.

5. Conclusions

The vertical TKE profiles in a system with a submerged rigid canopy submitted to turbulence generated by an oscillating grid were divided into three zones: one above the canopy and two inside the canopy. Above the canopy, the TKE found for all SPFs was greater than in those zones without any vegetation. This phenomenon was attributed to the redistribution of TKE at a lower volume, enhanced mainly by the largest SPFs.

The inner zone nearer the top of the canopy is called the transition zone. Although it was situated inside the plants, the TKE was still greater than that found without any plants. The third zone is situated below the transition zone and is defined as the region where the TKE was lower than TKE found in 'unvegetated' experiments. This phenomenon was called sheltering or dampening, and along with the depth of the transition zone was enhanced with a decrease in the stem diameter and an increase in the SPF of the canopies that caused a reduction in the plant-to-plant distance. We have, therefore, not only observed a sheltering, but quantified it. The development of the sheltering was reduced as frequency increased, due to the fact that vegetation could not prevent the penetration of the turbulence.

The semi-rigid model canopies prevented the development of a transitional zone, and a steep gradient of TKE above and inside the canopy was found. This process can be attributed to the morphology of the semi-rigid canopy, which produced a major increase in the SPF at the top of the canopy, since the distribution of the vertical biomass was not uniform. The experiments with SAV revealed that the transitional zone disappeared due to the

layout of the leaves, which isolated the two zones. The movement of the real plants contributed to enhancing the sheltering and reducing the transitional zone. As the frequency increased, the sheltering intensified because there was greater movement of the plants at the top, thus incrementing the attenuation of the turbulence inside the canopy.

Acknowledgements

This research was funded by the *Ministerio de Educación y Cultura* of the Spanish Government through grant CGL 2007-62483/HID to the University of Girona. Dolors Pujol was supported by research fellowship BR08/11 of the University of Girona. The cost of the article publication was subsidized by a grant of the University of Girona. We would like to acknowledge the contributions of Xicu Gómez and Teresa Martí of the Department of Physics at the University of Girona and Amélie Dasre from the *Institut Universitaire et Technologique du Creusot* (France).

References

Ackerman, J.D., Okubo, A., 1993. Reduced mixing in a marine macrophyte canopy. Funct. Ecol. 7, 305–309.

Begon, M., Harper, J.L., Townsend, C.R., 1986. Ecology: Individuals, Populations and Communities 1st ed. Blackwell Science, Oxford.

Bouma, T.J., van Duren, L.A., Temmerman, S., Claverie, T., Blanco-Garcia, A., Ysebaert, T., Herman, P.M.J., 2007. Spatial flow and sedimentation patterns within patches of epibenthic structures: Combining field, flume and modelling experiments. Cont. Shelf Res. 27, 1020–1045.

Brooks, R., 1989. An overview of ecological functions and economic values of wetlands, in: Majumdar, S., Brooks, R., Brenner, F., Tiner, R. (Eds.), Wetlands Ecology and Conservation: Emphasis in Pennsylvania. The Pennsylvania Academy of Science, New Jersey, pp. 11–20.

Brumley, B.H., Jirka, G.H., 1987. Near-surface turbulence in a grid-stirred tank. J. Fluid Mech. 183, 235–263.

Christiansen, T., Wiberg, P.L., Milligan, T.G., 2000. Flow and sediment transport on a tidal salt marsh surface. Estuar. Coast Shelf. 50, 315–331.

Connolly, J.P., Armstrong, N.E., Miksad, R.W., 1983. Adsorption of hydrophobic pollutants in estuaries. J. Environ. Eng-Asce. 109, 17–35.

Desilva, I.P.D., Fernando, H.J.S., 1994. Oscillating grids as a source of nearly isotropic turbulence. Phys. Fluids 6, 2455–2464.

Gambi, M.C., Nowell, A.R.M., Jumars, P.A., 1990. Flume observations on flow dynamics in Zostera marina (eelgrass) beds. Mar. Ecol. Prog. Ser. 61, 159–169.

Ghisalberti, M., Nepf, H., 2006. The structure of the shear layer in flows over rigid and flexible canopies. Environ. Fluid Mech. 6, 277–301.

Gorham, E., 1991. Northern peatlands: role in the carbon cycle and probable responses to climatic warming. Ecol. Appl. 1, 182–195.

Holzner, M., Liberzon, A., Guala, M., Tsinober, A., Kinzelbach, W., 2006. Generalized detection of a turbulent front generated by an oscillating grid. Exp. Fluids 41, 711–719.

Hopfinger, E.J., Toly, J.A., 1976. Spatially decaying turbulence and its relation to mixing across density interfaces. J. Fluid Mech. 78, 155–175.

Jarvela, J., 2002. Flow resistance of flexible and stiff vegetation: a flume study with natural plants. J. Hydrol. 269, 44–54.

Kline, S.J., McClintock, F.A., 1953. Describing the uncertainties in single-sample experiments. Mech. Eng. 75, 3–8.

Koch, E.W., Gust, G., 1999. Water flow in tide- and wave-dominated beds of the seagrass Thalassia testudinum. Mar. Ecol. Prog. Ser. 184, 63–72.

Leonard, L.A., Croft, A.L., 2006. The effect of standing biomass on flow velocity and turbulence in Spartina alterniflora canopies. Estuar. Coast. Shelf Sci. 69, 325–336.

Leonard, L.A., Luther, M.E., 1995. Flow hydrodynamics in tidal marsh canopies. Limnol. Oceanogr. 40, 1474–1484.

Leonard, L.A., Reed, D.J., 2002. Hydrodynamics and sediment transport through tidal marsh canopies. J. Coast. Res. 36, 459–469.

Machate, T., Noll, H., Behrens, H., Kettrup, A., 1997. Degradation of phenanthrene and hydraulic characteristics in a constructed wetland. Water Res. 31 554–560

Matsunaga, N., Sugihara, Y., Komatsu, T., Masuda, A., 1999. Quantitative properties of oscillating-grid turbulence in a homogeneous fluid. Fluid Dyn. Res. 25 147–165

Mazzella, L., Alberte, R.S., 1986. Light adaptation and the role of autotrophic epiphytes in primary production of the temperate seagrass, Zostera marina L. J. Exp. Mar. Biol. Ecol. 100, 165–180.

Morris, E.P., Peralta, G., Brun, F.G., van Duren, L., Bouma, T.J., Perez-Llorens, J.L., 2008. Interaction between hydrodynamics and seagrass canopy structure: spatially explicit effects on ammonium uptake rates. Limnol. Oceanogr. 53, 1531–1539.

Nepf, H.M., 1999. Drag, turbulence, and diffusion in flow through emergent vegetation. Water Resour. Res. 35, 479–489.

Nepf, H.M., Vivoni, E.R., 2000. Flow structure in depth-limited, vegetated flow. J. Geophys. Res. 105, 28547–28557.

Neumeier, U., 2007. Velocity and turbulence variations at the edge of saltmarshes. Cont. Shelf Res. 27, 1046–1059.

Neumeier, U., 2005. Quantification of vertical density variations of salt-marsh vegetation. Estuar. Coast. Shelf Sci. 63, 489–496.

Neumeier, U., Amos, C.L., 2006. The influence of vegetation on turbulence and flow velocities in European salt-marshes. Sedimentology 53, 259–277.

Neumeier, U., Ciavola, P., 2004. Flow resistance and associated sedimentary processes in a Spartina maritima salt-marsh. J. Coast. Res. 20, 435–447.

Nokes, R.I., 1988. On the entrainment rate across a density interface. J. Fluid Mech. 188, 185–204.

Orlins, J.J., Gulliver, J.S., 2003. Turbulence quantification and sediment resuspension in an oscillating grid chamber. Exp. Fluids 34, 662–677.

Peralta, G., van Duren, L.A., Morris, E.P., Bouma, T.J., 2008. Consequences of shoot density and stiffness for ecosystem engineering by benthic macrophytes in flow dominated areas: a hydrodynamic flume study. Mar. Ecol. Prog. Ser. 368, 103–115.

Poggi, D., Katul, G.G., Albertson, J.D., 2004. Momentum transfer and turbulent kinetic energy budgets within a dense model canopy. Bound.-Layer Meteorol. 111, 589–614.

Prigent, C., Matthews, E., Aires, F., Rossow, W.B., 2001. Remote sensing of global wetland dynamics with multiple satellite data sets. Geophys. Res. Lett. 28, 4631–4634.

Raupach, M.R., Thom, A.S., 1981. Turbulence in and above plant canopies. Annu. Rev. Fluid Mech. 13, 97–129.

Sand-Jensen, K., Pedersen, O., 1999. Velocity gradients and turbulence around macrophyte stands in streams. Freshwater Biol. 42, 315–328.

Serra, T., Colomer, J., Logan, B.E., 2008. Efficiency of different shear devices on flocculation. Water Res. 42, 1113–1121.

Serra, T., Fernando, H.J.S., Rodriguez, R.V., 2004. Effects of emergent vegetation on lateral diffusion in wetlands. Water Res. 38, 139–147.

Shi, Z., Hughes, J.M.R., 2002. Laboratory flume studies of microflow environments of aquatic plants. Hydrol. Processes 16, 3279–3289.

Shi, Z., Pethick, J.S., Pye, K., 1995. Flow structure in and above the various heights of a saltmarsh canopy: a laboratory flume study. J. Coast. Res. 11, 1204–1209.

Willems, H.P.L., Rotelli, M.D., Berry, D.F., Smith, E.P., Reneau, R.B., Mostaghimi, S., 1997. Nitrate removal in riparian wetland soils: effects of flow rate, temperature, nitrate concentration and soil depth. Water Res. 31, 841–849.

Yang, S.L., 1998. The role of Scirpus marsh in attenuation of hydrodynamics and retention of fine sediment in the Yangtze estuary. Estuar. Coast. Shelf Sci. 47, 227–233.